Chemical Science

ROYAL SOCIETY OF CHEMISTRY

EDGE ARTICLE

View Article Online
View Journal | View Issue

Cite this: *Chem. Sci.*, 2021, **12**, 12806

All publication charges for this article have been paid for by the Royal Society of Chemistry

On-surface synthesis of organocopper metallacycles through activation of inner diacetylene moieties†

Borja Cirera,[a] Alexander Riss,[b] Pingo Mutombo,[c] José I. Urgel,[ad] José Santos,[ae] Marco Di Giovannantonio,[df] Roland Widmer,[d] Samuel Stolz,[dg] Qiang Sun,[d] Max Bommert,[d] Roman Fasel,[dh] Pavel Jelínek,*[c] Willi Auwärter,*[b] Nazario Martín *[ae] and David Écija *[a]

Received 7th July 2021
Accepted 28th August 2021

DOI: 10.1039/d1sc03703j

rsc.li/chemical-science

The design of organometallic complexes is at the heart of modern organic chemistry and catalysis. Recently, on-surface synthesis has emerged as a disruptive paradigm to design previously precluded compounds and nanomaterials. Despite these advances, the field of organometallic chemistry on surfaces is still at its infancy. Here, we introduce a protocol to activate the inner diacetylene moieties of a molecular precursor by copper surface adatoms affording the formation of unprecedented organocopper metallacycles on Cu(111). The chemical structure of the resulting complexes is characterized by scanning probe microscopy and X-ray photoelectron spectroscopy, being complemented by density functional theory calculations and scanning probe microscopy simulations. Our results pave avenues to the engineering of organometallic compounds and steer the development of polyyne chemistry on surfaces.

Introduction

Organocopper compounds play a pivotal role in organic synthesis, for instance in conjugate addition reactions and couplings with sp^2 carbons, while also promoting epoxide openings, S_N2 and S_N2' reactions, and alkyne additions, just to name a few. Notably, based on this chemical relevance, the demand for organocopper complexes is increasing due to the low cost and environmental friendliness of copper.[1]

Recently, on-surface synthesis has emerged as a discipline that allows the design of chemical products, while providing access to surface science techniques to explore materials with utmost spatial resolution.[2–6]

By taking advantage of this novel synthetic paradigm, organocopper complexes have been designed by exploiting halogen-substituted compounds, typically as intermediates of the Ullmann coupling reaction. Most of the focus has been centered on halogenated sp^2 carbons, with scarce examples reporting the formation of organometallic polyyne nanostructures *via* the chemical reactions of brominated or hydrogenated sp carbons.[7–12]

In parallel, terminal acetylene on-surface chemistry has shown promising results towards the fabrication of well-defined low-dimensional nanomaterials,[2,6] illustrating distinct reactions such as Glaser coupling,[13–15] head to head addition,[16,17] alkyne cyclotrimerization,[18,19] Bergmann reaction,[20,21] azide–alkyne cycloaddition,[22,23] Sonogashira coupling[24,25] and dehalogenative homocoupling.[26]

Inspired by this previous knowledge, here we introduce a new pathway to activate inner polyyne moieties affording the formation of unprecedented organocopper metallacycles. To this aim we deposit the precursor 1,4-di(naphthalen-2-yl)butadi-1,3-yne (**1**), termed **DNBD**, on Cu(111) held at room temperature. Such species incorporate an inner 1,3-butadiyne moiety that is connected at both termini to rotatable naphthalene moieties. Our scanning probe microscopy (SPM) study complemented by X-ray photoelectron spectroscopy (XPS), density functional theory (DFT) and scanning probe microscopy calculations reveals that the two exterior carbon atoms of the

[a]*IMDEA Nanoscience, C/Faraday 9, Campus de Cantoblanco, 28049 Madrid, Spain. E-mail: david.ecija@imdea.org*

[b]*Physics Department E20, Technical University of Munich, D-85748 Garching, Germany. E-mail: wau@tum.de*

[c]*Institute of Physics of the Czech Academy of Science, 16253 Praha, Czech Republic. E-mail: jelinekp@fzu.cz*

[d]*Empa, Swiss Federal Laboratories for Materials Science and Technology, 8600 Dübendorf, Switzerland*

[e]*Departamento de Química Orgánica, Facultad de Ciencias Químicas, Universidad Complutense de Madrid, 28040 Madrid, Spain. E-mail: nazmar@quim.ucm.es*

[f]*Istituto di Struttura della Materia – CNR (ISM-CNR), via Fosso del Cavaliere 100, 00133 Roma, Italy*

[g]*Institute of Physics, École Polytechnique Fédérale de Lausanne, CH-1015 Lausanne, Switzerland*

[h]*Department of Chemistry, Biochemistry and Pharmaceutical Sciences, University of Bern, 3012 Bern, Switzerland*

† Electronic supplementary information (ESI) available. See DOI: 10.1039/d1sc03703j

diacetylene skeleton of **DNBD** are attacked by copper adatoms resulting in the synthesis of organocopper metallacycles, through the transformation of the diacetylene moiety of the precursors into a cumulene-like structure. Our results pave avenues for the activation of carbons on metal surfaces, giving rise to the design of unique organometallic complexes of potential relevance for modern organic synthesis and catalysis.

Results and discussion

The synthesis of molecular species **1** (*cf.* the left panel of Fig. 1a and S1† for synthetic details) was conceived to equip a diacetylene moiety with protecting naphthalene units at its termini, which are able to rotate through a single bond, thus featuring two conformers upon adsorption, named *s-cis* and *s-trans* (*cf.* the left panel of Fig. 1a). Thanks to that geometrical flexibility we envisioned that the carbon atoms involved in the butadiene bridge could be easily attacked by metal adatoms on specific coinage surfaces (*cf.* the right panel of Fig. 1a). To this aim, the behavior of the molecular precursor was inspected on surfaces with low and high reactivity, *i.e.*, Au(111) and Cu(111), respectively.

First, the deposition of **DNBD** on Au(111) held at room temperature results in the formation of chain-like nanostructures that evolve towards a closely packed assembly upon high coverage, stabilized through van der Waals interactions (*cf.* the left panel of Fig. 1b and S2a–d†). Importantly, high resolution images allow us to discern the intact species featuring *s-cis* or *s-trans* isomers, whereas the *s-trans* is in the majority (>90%). Consecutive annealing steps up to 650 K give rise to the formation of irregularly polymerized species, signaling uncontrolled reaction pathways (*cf.* Fig. S2e and f†).

The above mentioned scenario changes dramatically when **DNBD** is deposited on the more reactive Cu(111) held at room temperature. As illustrated in Fig. 2, a submonolayer coverage results in the expression of cross-like entities (*cf.* right panel of Fig. 1b, 2a and b) which are visualized in constant-current STM as two central lobes surrounded by four elongated protrusions, which can have distinct relative orientations. Such entities are rationalized as cumulene-based organocopper metallacycles (**2**), the formation of which is tentatively explained thanks to a mechanism by which the inner triple bonds of the diacetylene bridges react with copper adatoms. The organometallic complexes can adopt six different conformations (*cf.* Fig. 2c–h), with associated chiral ones with respect to the substrate. As depicted in the histogram in Fig. 2i, three conformers occur much more frequently. Notably, the longitudinal axis of symmetry of the macrocycle is aligned with the close-packed directions of Cu(111). The robustness of the organocopper metallacycles is confirmed by performing lateral manipulation, revealing that the complexes can be displaced and rotated along the surface over long distances (*cf.* Fig. 2j and k). In addition, a scanning probe microscopy image acquired at 77 K shows that they diffuse as a whole along the close-packed directions of the surface (*cf.* Fig. 2l). Such findings corroborate the formation of two relatively strong C–Cu–C bonds per organometallic complex.

In order to get more information about the chemical structure of the organocopper metallacycle, we performed high-resolution X-ray photoelectron spectroscopy (HR-XPS) using synchrotron radiation as the photon source. The C 1s core level of a sample with a coverage of 0.4 ML is shown in Fig. 2m. The carbon atoms contained in complex **2** appear in different chemical environments: 4 are bound to Cu adatoms, 4 constitute the cumulene bridges (with sp hybridization), 12 are connected to other carbon atoms only, with sp^2 hybridization, and 28 are linked to hydrogens. Deconvolution of the C 1s signal has been performed by fixing these relative ratios, which produces the fit reported in Fig. 2m that is in very good agreement with the experimental data. The components related to C–H and C–C in the sp^2 hybridized moieties (blue and green filled curves in Fig. 2m) appear at 284.1 eV and 284.6 eV, respectively,[27] while the carbon atoms in the sp cumulene moieties (orange filled curve in Fig. 2m) display a spectroscopic signal at higher binding energy (285.1 eV). It must be noted that a fit without a separate component arising from the sp cumulene moieties did not satisfactorily reproduce the experimental data (see Fig. S3†). Interestingly, the component at lower binding energy (283.5 eV, purple filled curve in Fig. 2m) confirms the presence of metal-bound carbon atoms, as previously reported.[27,28]

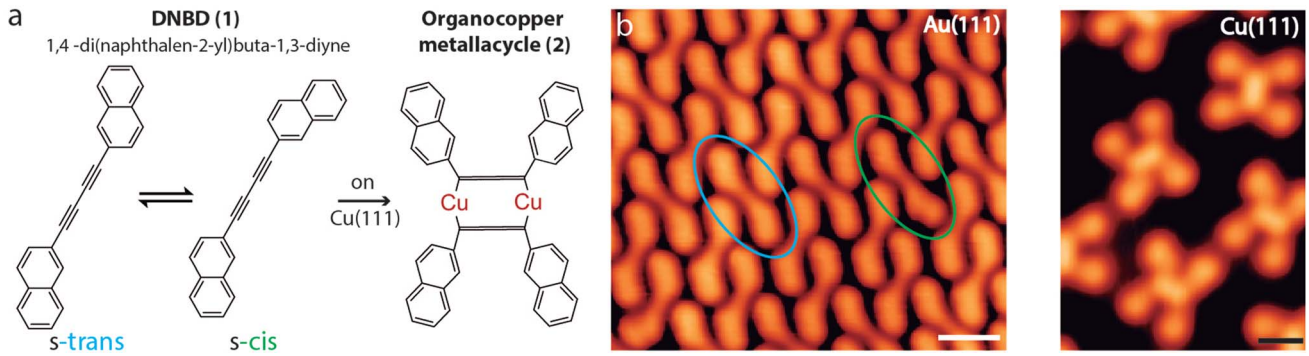

Fig. 1 Conformations, self-assembly and transformations of **DNBD** species on Au(111) and Cu(111). (a) Chemical scheme of the **DNBD** conformers (**1**) and organocopper metallacycles (**2**). (b) High resolution STM image of the **DNBD** conformers on Au(111) and the organometallic cycles (**2**) on Cu(111). Au(111): $I_t = 120$ pA, $V_b = -0.25$ V, scale bar = 1 nm; Cu(111): $I_t = 500$ pA, $V_b = -1.5$ V, scale bar = 1 nm.

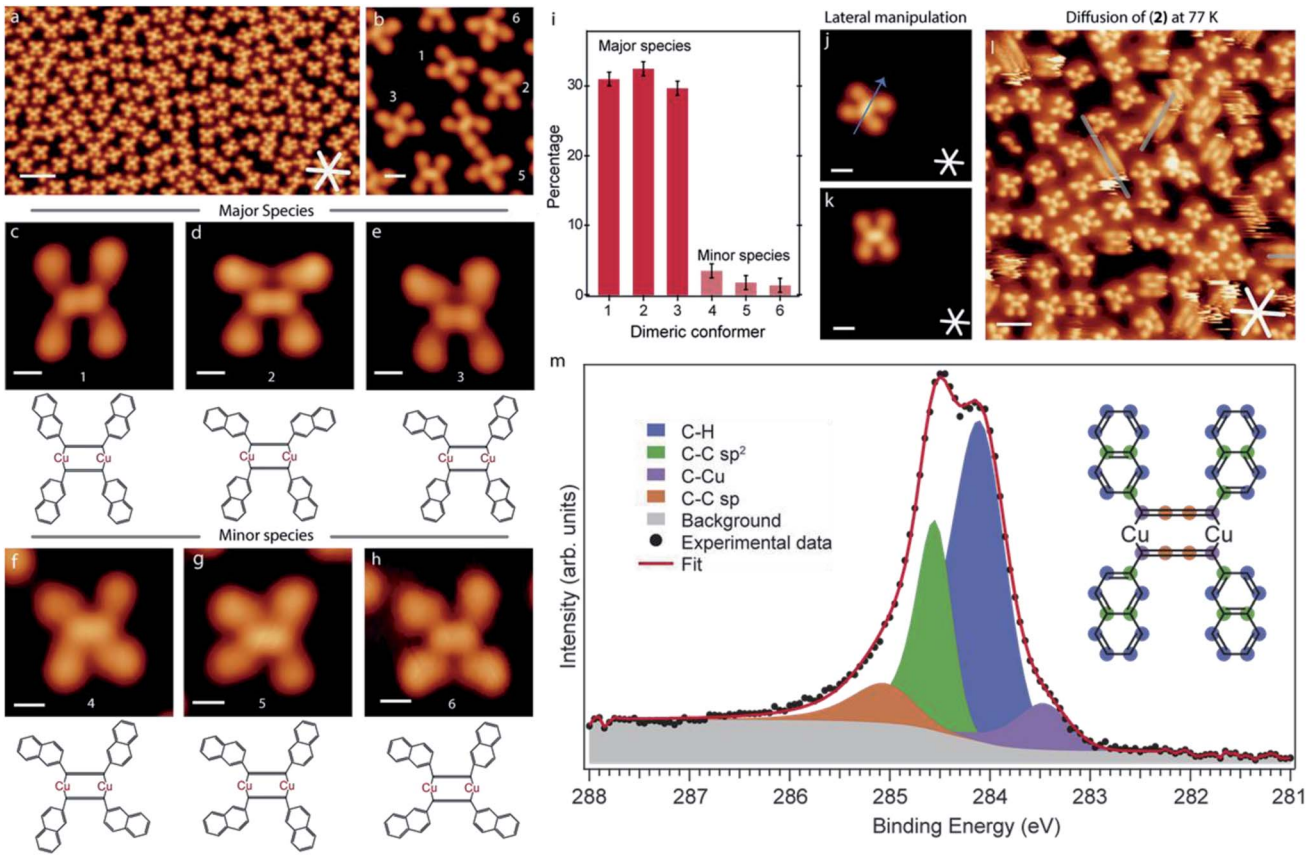

Fig. 2 Formation and robustness of organocopper metallacycles. (a) Large-scale STM image of **DNBD** species deposited on Cu(111) held at room temperature. Numerous four-lobed species of dissimilar conformations can be observed (scale bar = 5 nm, $I_t = 100$ pA, $V_b = -1.0$ V). (b) Zoom-in region showing distinct conformers of the organocopper metallacycles (scale bar = 5 Å, $I_t = 500$ pA, $V_b = -1.5$ V). (c–e) The three major conformers of **2** (scale bar = 5 Å, $I_t = 200$ pA, $V_b = -0.1$ V). (f–h) The three minor conformers of **2** (scale bar = 5 Å; (f): $I_t = 200$ pA, $V_b = -0.7$ V; (g): $I_t = 200$ pA, $V_b = 0.5$ V; (h): $I_t = 500$ pA, $V_b = -1.5$ V). (i) Statistical distribution based on experimental results, showing a stark contrast between the amounts of 1, 2, 3 conformers compared to those of 4, 5, 6 ones. (j and k) *In situ* lateral manipulation of complex **2** as a single unit, where the tip pathway is depicted with a blue arrow (scale bar = 1 nm, $I_t = 175$ pA, $V_b = -1.0$ V; manipulation parameters: $I_t = 25$ nA, $V_b = -100$ mV). (l) STM image at 77 K showing the diffusion of the organocopper metallacycles along the high-symmetry directions of the underlying Cu(111) (scale bar = 2.5 nm, $I_t = 10$ pA, $V_b = -0.5$ V). (m) High-resolution XPS spectrum of the C 1s core level acquired using synchrotron radiation with a photon energy of 425 eV after deposition of 0.4 ML coverage of **DNBD** on Cu(111) held at RT. Colored dots in the scheme highlight carbon atoms in different chemical environments, and their colors correspond to those of the fitting components. Fitting parameters are reported in Table S1.†

Next, to shed light on the nature of the organocopper metallacycles, we investigated them simultaneously with scanning tunneling and non-contact atomic force microscopies (nc-AFM). First, we deposited **DNBD** on submonolayer patches of NaCl on Cu(111) held at 30 K in order to ensure its adsorption on ultrathin films. Fig. 3a and b illustrate that on NaCl, where no copper adatoms are available, individual species are found. The naphthalene moieties are clearly distinguished, while the inner bridge shows two bright protrusions in nc-AFM, which is a fingerprint of the triple bond character, thus confirming the preservation of the diacetylene bridge.[8,29] Second, we inspected complex **2** formed by depositing the precursors on Cu(111) held at room temperature. The naphthalene moieties are clearly visible (*cf.* Fig. 3c and d), whereas the macrocycle of the complex does not show any fingerprint of the previous triple bonds, signaling the change of the carbon hybridization. Instead, two bent lines can be observed, which are associated with a distortion of the cumulene bridge due to interaction with the substrate (*cf.* Fig. 3e and S4†). The C–Cu–C is seen as a straight line, in agreement with recently reported organometallic systems on Cu(111).[9,11] Our experimental interpretation of complex **2** is qualitatively well corroborated by STM and nc-AFM simulations of a DFT relaxed organocopper metallacycle on the surface (*cf.* Fig. 4). The STM simulated images display the characteristic double protrusion of the macrocycle visualized with STM at biases of distinct polarity. In addition, the match between the experimental nc-AFM image (*cf.* Fig. 3d and e) and the simulation (*cf.* Fig. 4d) is good, being able to reproduce the bend of the cumulene-like bridge for close enough tip-sample distance (*cf.* inset of Fig. 4d). All conformers inspected with the nc-AFM exhibited this behavior (*cf.* Fig. S4†).

Notably, according to our rationalization, due to the formation of the organocopper metallacycles, there is an unprecedented transformation from sp to sp^2 hybridization of the butadiyne precursors, giving rise to cumulene-like bridges. A possible transformation route could be initiated by the attack of

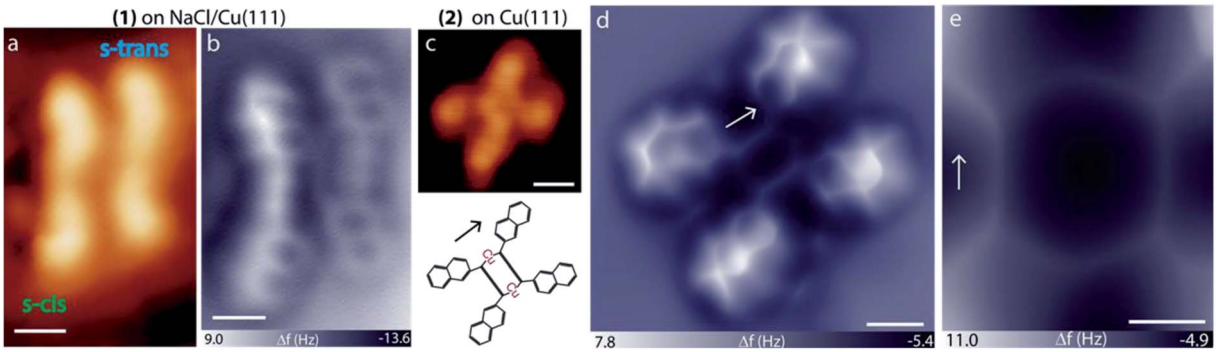

Fig. 3 Non-contact AFM characterization of species **1** and organometallic complex **2**. (a and b) STM and nc-AFM images of *cis*- and *trans*-**DNBD** conformers, adsorbed on NaCl held at 30 K. The triple bonds are visualized as bright protrusions. (a) Scale bar = 3 Å, I_t = 5 pA, V_b = 100 mV. (b) Scale bar = 5 Å. (c) STM image of organocopper complex **2** on Cu(111), formed by depositing the **DNBD** species at room temperature, with the corresponding model (scale bar = 1 nm, I_t = 13 pA, V_b = 100 mV). (d) Non-contact AFM image of complex **2** reproduced in (c). Scale bar = 5 Å. (e) Zoom-in non-contact AFM image of the organocopper metallacycle. Scale bar = 2 Å. The white arrows in (d) and (e) are a guide to the eye and oriented in the same direction with respect to the molecule.

a copper adatom to the carbon belonging to the triple C–C bond of a single **DNBD** species, where the electron density is augmented, as illustrated in Fig. S5.†

Importantly, the Bader analysis of the charges of complex **2** reveals that each copper adatom loses $0.18e^-$, and thus they could be considered as Cu(0), which is remarkable since most of the organometallic copper compounds are in the Cu^{1+} oxidation state.[1]

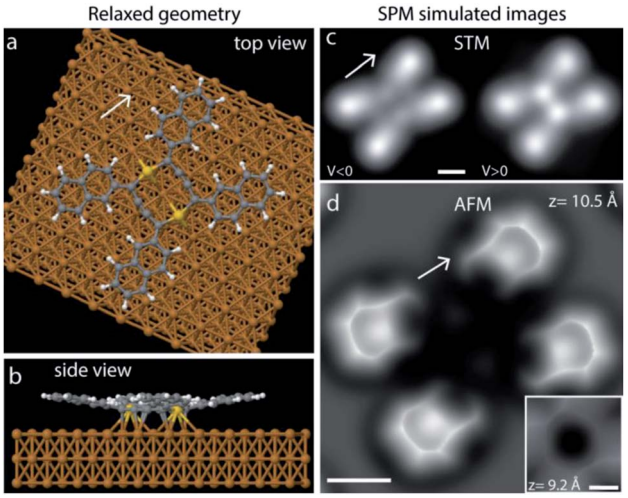

Fig. 4 Theoretical modelling of the organocopper metallacycle. (a and b) Top- and side-view of complex **2** displaying the DFT-relaxed geometry in a stick-and-ball representation. Within the metallacycle, the Cu adatoms are located 2.00 Å over the surface, whereas the C atoms comprising the cumulene-like bridge are positioned between 2.00 and 2.07 Å over Cu(111). White, grey, and orange balls represent hydrogen, carbon and copper atoms, respectively. Yellow balls display copper adatoms. (c) STM simulated image of complex **2** for negative and positive bias. Scale bar = 5 Å. (d) Non-contact AFM simulated image of the organocopper metallacycle depicted in (a). Scale bar = 5 Å. The white arrows are a guide to the eye to relate the relaxed geometry and the SPM simulated images with the experimental findings in Fig. 3. Inset: non-contact AFM simulated image of the organocopper metallacycle at a lower tip–sample distance, reproducing the bend of the cumulene-like bridge. Scale bar = 2 Å.

Conclusions

In summary, we described the synthesis, adsorption and chemical conversion of **DNBD** species on coinage metal surfaces. Such molecular precursors are based on a diacetylene linker joined at its periphery by naphthalene moieties in order to steer molecular flexibility, which facilitates the reaction of the triple bonds with metal adatoms on reactive surfaces.

On the weakly interacting Au(111) and NaCl/Cu(111) substrates, the molecular species remain pristine. On Au(111) further annealing of the sample does not promote any discernible reaction product.

In sharp contrast, on the more reactive Cu(111) substrate, **DNBD** species undergo a chemical attack by the copper adatoms yielding the formation of robust organocopper metallacycles based on cumulene-like bridges featuring a rare Cu(0) oxidation state. Thus, our results illustrate an unprecedented chemical reaction on a metallic surface and provide pathways to engineer robust organocopper complexes and to develop the on-surface chemistry of copper and cumulene compounds.

Experimental and theoretical methods

Growth and scanning probe microscopy characterization

STM characterization was performed in two independent ultra-high vacuum systems with base pressures below 5×10^{-10} mbar, hosting a Createc and an Omicron low-temperature scanning tunneling microscope, respectively. All images were taken in constant-current mode unless stated otherwise, with electrochemically etched tungsten tips, applying a bias (V_b) to the sample and at a temperature of ≈4 K, unless stated differently. Non-contact AFM measurements were performed at constant height and at V_b = 0 V using a qPlus sensor (resonance frequency ≈ 30 kHz, Q value = 70 000, oscillation amplitude = 60 pm) with CO-functionalized tips. The Au(111) and Cu(111) substrates were prepared by cycles of Ar+ sputtering (800 eV) and subsequent annealing to 723 and 823 K for 10 minutes, respectively. NaCl and **DNBD** were deposited from Knudsen

cells ($T_{NaCl} = 800$ K and $T_{DNBD} = 385$ K) onto the substrates held at room temperature.

X-ray photoelectron spectroscopy

XPS measurements were performed at the X03DA beamline (PEARL endstation)[30] at the SLS synchrotron radiation facility (Villigen, Switzerland), using linearly (and partially circularly left/right) polarized radiation with a photon energy of 425 eV. XPS spectra were obtained in normal emission geometry, using an R4000 hemispherical electron analyzer from Scienta equipped with a multichannel plate (MCP) detector, and recorded at room temperature in "swept" mode with 20 eV pass energy.

Density functional theory calculations

We performed density functional theory calculations as implemented in the FHI-aims code[31] in order to study the interaction between the molecular species and the Cu(111) surface. The calculations were carried out using the GGA-PBE approximation of the exchange–correlation potential including the Tkatchenko–Scheffler treatment of the van der Waals interactions.[32]

The Cu(111) surface was modeled using a 10×10 supercell made of three layers. Different starting configurations of the molecule on the surface were investigated. The structural optimization was performed until the total energy and the remaining atomic forces were below 10^{-5} eV and 10^{-2} eV Å^{-1}, respectively. All the atoms of the supercell were thoroughly relaxed, except the bottom Cu layer. A single gamma point was used for the integration of the Brillouin zone. The calculated Hartree potential and the total charge density were used to determine the electronic properties of the molecule on the surface.

AFM simulations

AFM image simulations were performed using the ProbeParticle code,[33,34] which takes into account the van der Waals (vdW) and the electrostatic interactions between the CO tip and the surface. The Lennard–Jones potential was used to describe the van de Waals interactions. The Hartree potential used to calculate the electrostatic forces and Pauli repulsion were obtained from DFT calculations. All simulations were done with an effective charge of $-1e$ and a lateral stiffness of $k = 0.25$ N m^{-1}.

Data availability

Data of this study are available from the corresponding author upon reasonable request.

Author contributions

B. C., N. M. and D. E. conceived the project. B. C. and D. E. performed the STM measurements. B.C., A. R. and W. A. acquired the nc-AFM images. P. M. and P. J. performed the DFT calculations and the nc-AFM simulations. J. I. U., M. G., R. W., S. S., Q. S., and M. B. acquired the XPS data. J. S. and N. M. synthesized the chemical precursors. B. C., A. R., P. M., J. I. U., M. G., R. F., P. J., W. A., N. M. and D. E. analyzed the data, which were discussed with all the authors. B. C., J. I. U., P. J., W. A., N. M. and D. E. wrote the paper with contributions from all the authors.

Conflicts of interest

There are no conflicts to declare.

Acknowledgements

We acknowledge the Comunidad de Madrid [project QUIMTRONIC-CM (Y2018/NMT-4783)], the EC FP7-PEOPLE-2011-COFUND AMAROUT II, and Ministerio de Ciencia e Innovación (PID2019-108532GB-I00). IMDEA Nanociencia thanks support from the "Severo Ochoa" Programme for Centers of Excellence in R&D (MINECO, Grant SEV-2016-0686). P.J. acknowledges support from Praemium Academie of the Academy of Science of the Czech Republic, GACR 18-09914S. Computational resources were provided by the CESNET LM2015042 and the CERIT Scientific Cloud LM2015085. J.I.U. thanks the JCB Atracción de Talento program from Comunidad de Madrid (contract no. IND-12535). The XPS experiments were performed at the X03DA (PEARL) beamline at the Swiss Light Source, Paul Scherrer Institut, Villigen, Switzerland. We thank the beamline manager Dr Matthias Muntwiler (PSI) for his technical support.

References

1 *Modern Organocopper Chemistry*, ed. N. Krause, Wiley-VCH Verlag GmbH, 2002.
2 Q. Shen, H.-Y. Gao and H. Fuchs, Frontiers of on-surface synthesis: From principles to applications, *Nano Today*, 2017, **13**, 77–96.
3 N. Pavliček and L. Gross, Generation, manipulation and characterization of molecules by atomic force microscopy, *Nat. Rev. Chem.*, 2017, **1**, 0005.
4 Q. Zhong, X. Li, H. Zhang and L. Chi, Noncontact atomic force microscopy: Bond imaging and beyond, *Surf. Sci. Rep.*, 2020, **75**, 100509.
5 L. Grill and S. Hecht, Covalent on-surface polymerization, *Nat. Chem.*, 2020, **12**, 115–130.
6 Q. Sun, R. Zhang, J. Qiu, R. Liu and W. Xu, On-surface synthesis of carbon nanostructures, *Adv. Mater.*, 2018, **30**, 1705630.
7 L. Dong, P. N. Liu and N. Lin, Surface-activated coupling reactions confined on a surface, *Acc. Chem. Res.*, 2015, **48**, 2765–2774.
8 S. Kawai, O. Krejčí, A. S. Foster, R. Pawlak, F. Xu, L. Peng, A. Orita and E. Meyer, Diacetylene linked anthracene oligomers synthesized by one-shot homocoupling of trimethylsilyl on Cu(111), *ACS Nano*, 2018, **12**, 8791–8797.
9 Q. Li, B. Yang, J. Björk, Q. Zhong, H. Ju, J. Zhang, N. Cao, Z. Shi, H. Zhang, D. Ebeling, A. Schirmeisen, J. Zhu and L. Chi, Hierarchical dehydrogenation reactions on a copper surface, *J. Am. Chem. Soc.*, 2018, **140**, 6076–6082.

10 R. Zhang, B. Xia, H. Xu and N. Lin, Identifying multinuclear organometallic intermediates in on-surface [2+2] cycloaddition reactions, *Angew. Chem., Int. Ed.*, 2019, **58**, 16485–16489.

11 M. Telychko, J. Su, A. Gallardo, Y. Gu, J. I. Mendieta-Moreno, D. Qi, A. Tadich, S. Song, P. Lyu, Z. Qiu, H. Fang, M. J. Koh, J. Wu, P. Jelínek and J. Lu, Strain-induced isomerization in one-dimensional metal–organic chains, *Angew. Chem., Int. Ed.*, 2019, **58**, 18591–18597.

12 X. Yu, X. Li, H. Lin, M. Liu, L. Cai, X. Qiu, D. Yang, X. Fan, X. Qiu and W. Xu, Bond-scission-induced structural transformation from cumulene to diyne moiety and formation of semiconducting organometallic polyyne, *J. Am. Chem. Soc.*, 2020, **142**, 8085–8089.

13 Y.-Q. Zhang, N. Kepčija, M. Kleinschrodt, K. Diller, S. Fischer, A. C. Papageorgiou, F. Allegretti, J. Björk, S. Klyatskaya, F. Klappenberger, M. Ruben and J. V. Barth, Homo-coupling of terminal alkynes on a noble metal surface, *Nat. Commun.*, 2012, **3**, 1286.

14 H.-Y. Gao, H. Wagner, D. Zhong, J.-H. Franke, A. Studer and H. Fuchs, Glaser Coupling at Metal Surfaces, *Angew. Chem., Int. Ed.*, 2013, **52**, 4024–4028.

15 B. Cirera, Y.-Q. Zhang, J. Björk, S. Klyatskaya, Z. Chen, M. Ruben, J. V. Barth and F. Klappenberger, Synthesis of extended graphdiyne wires by vicinal surface templating, *Nano Lett.*, 2014, **14**, 1891–1897.

16 A. Riss, A. P. Paz, S. Wickenburg, H.-Z. Tsai, D. G. De Oteyza, A. J. Bradley, M. M. Ugeda, P. Gorman, H. S. Jung, M. F. Crommie, A. Rubio and F. R. Fischer, Imaging single-molecule reaction intermediates stabilized by surface dissipation and entropy, *Nat. Chem.*, 2016, **8**, 678–683.

17 J. Lawrence, M. S. G. Mohammed, D. Rey, F. Aguilar-Galindo, A. Berdonces-Layunta, D. Peña and D. G. de Oteyza, Reassessing alkyne coupling reactions while studying the electronic properties of diverse pyrene linkages at surfaces, *ACS Nano*, 2021, **15**, 4937–4946.

18 J. Liu, P. Ruffieux, X. Feng, K. Müllen and R. Fasel, Cyclotrimerization of arylalkynes on Au(111), *Chem. Commun.*, 2014, **50**, 11200–11203.

19 H. Zhou, J. Liu, S. Du, L. Zhang, G. Li, Y. Zhang, B. Z. Tang and H.-J. Gao, Direct Visualization of surface-assisted two-dimensional diyne polycyclotrimerization, *J. Am. Chem. Soc.*, 2014, **136**, 5567–5570.

20 D. G. de Oteyza, P. Gorman, Y.-C. Chen, S. Wickenburg, A. Riss, D. J. Mowbray, G. Etkin, Z. Pedramrazi, H.-Z. Tsai, A. Rubio, M. F. Crommie and F. R. Fischer, Direct imaging of covalent bond structure in single-molecule chemical reactions, *Science*, 2013, **340**, 1434.

21 Q. Sun, C. Zhang, Z. Li, H. Kong, Q. Tan, A. Hu and W. Xu, On-surface formation of one-dimensional polyphenylene through Bergman cyclization, *J. Am. Chem. Soc.*, 2013, **135**, 8448–8451.

22 F. Bebensee, C. Bombis, S.-R. Vadapoo, J. R. Cramer, F. Besenbacher, K. V. Gothelf and T. R. Linderoth, On-surface azide–alkyne cycloaddition on Cu(111): Does it "click" in ultrahigh vacuum?, *J. Am. Chem. Soc.*, 2013, **135**, 2136–2139.

23 O. Díaz Arado, H. Mönig, H. Wagner, J.-H. Franke, G. Langewisch, P. A. Held, A. Studer and H. Fuchs, On-surface azide–alkyne cycloaddition on Au(111), *ACS Nano*, 2013, **7**, 8509–8515.

24 V. K. Kanuru, G. Kyriakou, S. K. Beaumont, A. C. Papageorgiou, D. J. Watson and R. M. Lambert, Sonogashira coupling on an extended gold surface in vacuo: Reaction of phenylacetylene with iodobenzene on Au(111), *J. Am. Chem. Soc.*, 2010, **132**, 8081–8086.

25 C. Sánchez-Sánchez, F. Yubero, A. R. González-Elipe, L. Feria, J. F. Sanz and R. M. Lambert, The flexible surface revisited: Adsorbate-induced reconstruction, momocoupling, and Sonogashira cross-coupling on the Au(100) surface, *J. Phys. Chem. C*, 2014, **118**, 11677–11684.

26 Q. Sun, L. Cai, H. Ma, C. Yuan and W. Xu, Dehalogenative homocoupling of terminal alkynyl bromides on Au(111): Incorporation of acetylenic scaffolding into surface nanostructures, *ACS Nano*, 2016, **10**, 7023–7030.

27 K. A. Simonov, N. A. Vinogradov, A. S. Vinogradov, A. V. Generalov, E. M. Zagrebina, G. I. Svirskiy, A. A. Cafolla, T. Carpy, J. P. Cunniffe, T. Taketsugu, A. Lyalin, N. Mårtensson and A. B. Preobrajenski, From graphene nanoribbons on Cu(111) to nanographene on Cu(110): Critical role of substrate structure in the bottom-up fabrication strategy, *ACS Nano*, 2015, **9**, 8997–9011.

28 M. Di Giovannantonio, M. El Garah, J. Lipton-Duffin, V. Meunier, L. Cardenas, Y. Fagot Revurat, A. Cossaro, A. Verdini, D. F. Perepichka, F. Rosei and G. Contini, Insight into organometallic intermediate and its evolution to covalent bonding in surface-confined Ullmann polymerization, *ACS Nano*, 2013, **7**, 8190–8198.

29 A. Sánchez-Grande, B. de la Torre, J. Santos, B. Cirera, K. Lauwaet, T. Chutora, S. Edalatmanesh, P. Mutombo, J. Rosen, R. Zbořil, R. Miranda, J. Björk, P. Jelínek, N. Martín and D. Écija, On-surface synthesis of ethynylene-bridged anthracene polymers, *Angew. Chem., Int. Ed.*, 2019, **58**, 6559–6563.

30 M. Muntwiler, J. Zhang, R. Stania, F. Matsui, P. Oberta, U. Flechsig, L. Patthey, C. Quitmann, T. Glatzel, R. Widmer, E. Meyer, T. A. Jung, P. Aebi, R. Fasel and T. Greber, Surface science at the PEARL beamline of the Swiss Light Source, *J. Synchrotron Radiat.*, 2017, **24**, 354–366.

31 V. Blum, R. Gehrke, F. Hanke, P. Havu, V. Havu, X. Ren, K. Reuter and M. Scheffler, Ab initio molecular simulations with numeric atom-centered orbitals, *Comput. Phys. Commun.*, 2009, **180**, 2175–2196.

32 A. Tkatchenko and M. Scheffler, Accurate molecular van der Waals interactions from ground-state electron density and free-atom reference data, *Phys. Rev. Lett.*, 2009, **102**, 073005.

33 P. Hapala, R. Temirov, F. S. Tautz and P. Jelínek, Origin of High-Resolution IETS-STM Images of organic molecules with functionalized tips, *Phys. Rev. Lett.*, 2014, **113**, 226101.

34 P. Hapala, G. Kichin, C. Wagner, F. S. Tautz, R. Temirov and P. Jelínek, Mechanism of high-resolution STM/AFM imaging with functionalized tips, *Phys. Rev. B: Condens. Matter Mater. Phys.*, 2014, **90**, 085421.